Bloch oscillations of Bose-Einstein condensates: Breakdown and revival

D. Witthaut, M. Werder, S. Mossmann, and H. J. Korsch*
FB Physik, Technische Universität Kaiserslautern, D-67653 Kaiserslautern, Germany
(Received 11 October 2004; published 30 March 2005)

We investigate the dynamics of Bose-Einstein condensates in a tilted one-dimensional periodic lattice within the mean-field (Gross-Pitaevskii) description. Unlike in the linear case the Bloch oscillations decay because of nonlinear dephasing. Pronounced revival phenomena are observed. These are analyzed in detail in terms of a simple integrable model constructed by an expansion in Wannier-Stark resonance states. We also briefly discuss the pulsed output of such systems for stronger static fields.

DOI: 10.1103/PhysRevE.71.036625 PACS number(s): 42.65.Tg, 03.75.Lm, 03.65.Nk, 42.50.Vk

I. INTRODUCTION

Despite its apparent simplicity, the dynamics of quantum particles in periodic structures is full of surprises, even in the one-dimensional case. Bloch waves, which are delocalized states in a lattice leading to transport, have been known for almost a century. If an additional static field F is introduced, these states become localized and counterintuitively transport is dramatically reduced. Instead an oscillatory motion is found, the famous Bloch oscillations. These have a (Bloch) frequency $\omega_B = Fd/\hbar$ where d is the lattice constant and they extend over a spatial interval Δ/F where Δ is the width of the first Bloch band. During the last decade these Bloch oscillations have been experimentally observed, which triggered a renewed theoretical interest (for recent reviews see [1–4]).

For stronger fields decay has to be taken into account. So this simple picture must be replaced by introducing couplings to higher bands or, alternatively, by a description in terms of Wannier-Stark resonances. More details can be found in the review article [5].

One of the most interesting systems for exploring the dynamics described above are cold atoms in optical lattices, because here the notorious difficulties met in solid state systems (where, in fact, the Bloch oscillations were observed for the first time [6]) are absent or, at least, can be made very small. Anderson and Kasevich did one of the first experiments [7] with a Bose-Einstein condensate (BEC) of rubidium atoms in an optical lattice with gravity acting as the static field. They could observe a pulsed coherent output of atoms.

The atoms in a BEC scatter off each other, which offers the opportunity to study the influence of the atomic interaction on the dynamics. In a good approximation, the dynamics can be described by the one-dimensional Gross-Pitaevskii equation (GPE) [8]

$$i\hbar\,\partial_t\psi = \left(-\frac{\hbar^2}{2M}\partial_x^2 + V(x) + Fx + g|\psi|^2\right)\psi, \qquad (1)$$

where M is the atomic mass, g is the interaction strength, and $V(x) = V(x+d)$ is the periodic lattice potential.

This nonlinear system shows basically all the features found in the analysis of the linear equation, such as Bloch oscillations of the condensate [9,10]. In addition, the nonlinearity introduces new effects, such as solitonlike motion, nonlinear Zener tunneling [11,12], and "classically" chaotic dynamics [13–15]. This system has been analyzed with various methods; see, e.g., [16–18].

Recent experiments demonstrated a breakdown of Bloch oscillations of a BEC in an optical lattice due to nonlinear interactions [19]. The dynamical instability disrupts the regular motion of Bloch oscillations whenever the BEC reaches the edge of the Brillouin zone. This instability is closely related to the nonlinear Zener tunneling discussed in Sec. II. However, in the experiment [19] as well as in corresponding theoretical studies [12,20–22], the mean-field potential $g|\psi(x)|$ is of the same strength as the optical lattice.

The present article focuses on Bloch oscillations in the regime where the mean-field potential is weak but not negligible in comparison to the periodic potential. In this situation nonlinear dephasing is the decisive mechanism causing a breakdown of Bloch oscillations. In fact we will show that the breakdown and other dynamical effects can be explained solely by nonlinear dephasing in a simple integrable model, which is introduced in Sec. III. Furthermore, revival phenomena are observed which obviously cannot be attributed to instability. Nevertheless dynamical instability cannot be entirely neglected. Preliminary numerical calculations show that it plays a role roughly at the same time scale as the dephasing leading to breakdown and revival. For example, the simple dephasing model predicts periodic revivals, but only the first one is actually observable (see Fig. 6 below). The interplay between dephasing and dynamical instability is subject to further studies.

The paper is organized as follows. In Sec. II we present results from a numerical solution of the GPE and show nonlinear Bloch oscillations for relatively weak fields and different strengths and signs of the nonlinear interaction. Section III introduces our main tool, a discrete representation by an expansion in Wannier-Stark resonance states and derives approximate results based on this approach. These results are used to analyze the dynamical behavior of Bloch oscillations in Sec. IV. Finally we discuss the modification of the coherent pulsed output of a Bloch oscillating condensate for stronger fields in Sec. V. The paper closes with some concluding remarks.

*Electronic address: korsch@physik.uni-kl.de

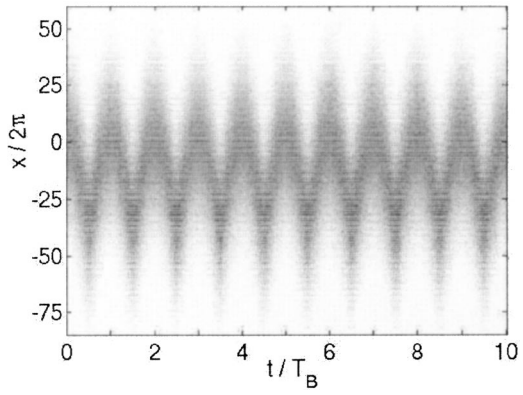

FIG. 1. The squared modulus $|\psi(x,t)|^2$ of the wave function for $g=0$ shows the familiar Bloch oscillations.

II. NUMERICAL STUDY OF NONLINEAR BLOCH OSCILLATIONS

Due to the nonlinearity of the GPE (1) analytical studies are difficult, so numerical simulations are helpful in guiding theoretical investigations.

In all numerical studies we will use a cosine potential $V(x)=V_0\cos(2\pi x/d)$. We furthermore use scaled units with $d=2\pi$, $V_0=M=1$ (see [5] for more details). It is worth noting that the scaled interaction strength is inversely proportional to the depth of the potential.

The GPE then reads

$$i\hbar\,\partial_t\psi=\left(-\frac{\hbar^2}{2}\partial_x^2+\cos x+Fx+g|\psi|^2\right)\psi \tag{2}$$

and we will use the value $\hbar=3.3806$ for the scaled Planck constant adapted to the experiment of Anderson and Kasevich [7] (see also [23]). The nonlinearity parameter is of the order $g\approx 1$ in this experiment. Here we will extend the analysis, however, to much stronger nonlinearities up to $|g|=10$. This regime could be reached experimentally by increasing the transverse confinement or decreasing the depth of the optical lattice.

Here we are mainly interested in the dynamics of Bloch oscillations and therefore use a weak field ($F=0.005$) and initial states populating almost exclusively the lowest Bloch band. In this case the decay is negligible. In the linear case the band gap between the lowest and the next higher Bloch band for the field-free case is $\delta=0.998$ and the probability

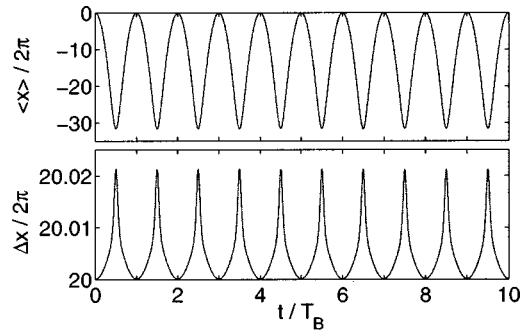

FIG. 2. Expectation values of the position $\langle x\rangle_t$ and width Δx_t for the wave function shown in Fig. 1.

for Zener tunneling is $\approx 10^{-12}$. As shown in [11,12], the tunneling probability is generally enhanced due to the nonlinearity. Furthermore, the tunneling probability does not vanish even for $F\to 0$, if the mean-field potential $g|\psi(x)|^2$ is of the same order of magnitude as the periodic potential $V(x)=\cos x$. As already mentioned we focus on the situation where the mean-field potential is weak but not negligible in comparison to the periodic potential. The Landau-Zener tunneling probability P calculated from a numerical propagation of the broad initial wave packet (3) showed that P increases slightly with $|g|$ but we still have $P<2\times 10^{-6}$ for $|g|\leqslant 10$. A significant increase of P was not observed until $|g|>30$. Hence nonlinear Landau-Zener tunneling does not play a role for the given parameters.

Let us start our discussion with a brief look at the Bloch oscillation for the linear case $g=0$. As an initial state, we use a Gaussian wave packet

$$\psi(x,t=0)=\frac{1}{(2\pi)^{1/4}\tilde{\sigma}^{1/2}}e^{-(x-x_0)^2/4\tilde{\sigma}^2} \tag{3}$$

with width $\tilde{\sigma}=40\pi$, which is projected onto the lowest Bloch band and afterward renormalized to unity. This wave packet contains no contributions from higher Bloch bands, which would decay rapidly (cf. the discussion in [1]). So the initial state closely resembles the state defined in Eq. (17), which is discussed in the context of the discrete model in Secs. III and IV.

For the time propagation a split-operator method [24] is used which can also be applied to the nonlinear case. In Fig. 1 we observe the familiar Bloch oscillation with a large am-

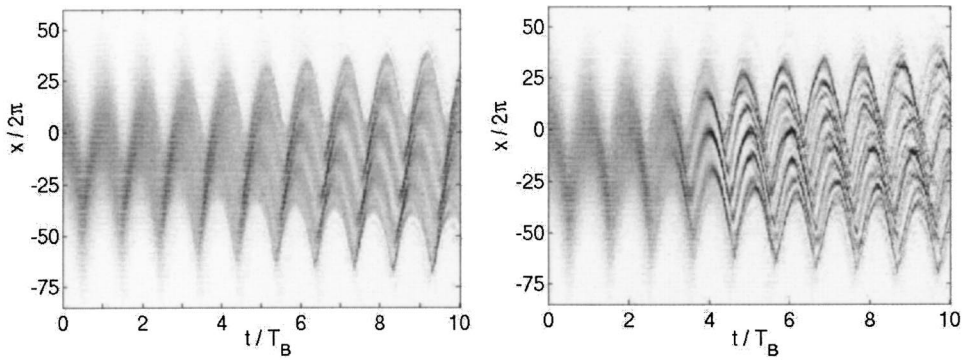

FIG. 3. Same as Fig. 1, but for a nonlinear interaction $g=+5$ (left) and -5 (right).

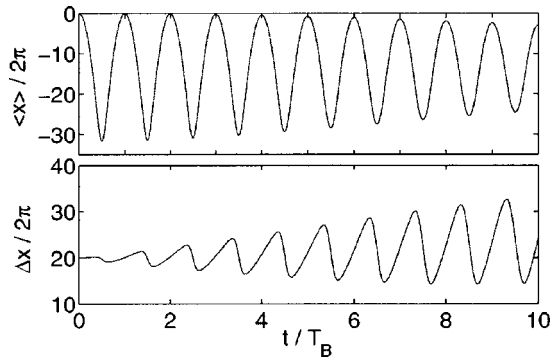

FIG. 4. Expectation values of the position $\langle x\rangle_t$ and width Δx_t for the wave function shown in Fig. 3 for a repulsive nonlinearity $g=+5$.

plitude because of the weak field. Let us recall that the region over which the Bloch oscillation extends can be estimated as $\Delta/F \approx 200 \approx 32\times 2\pi$ within the tilted band picture, where $\Delta=0.9994$ is the width of the dispersion relation $E(\kappa)$ in the field-free case. The numerical results confirm this estimate as the top of Fig. 2 shows. As expected for such an initially wide distribution in coordinate space, the width of the wave packet remains practically constant, varying periodically with a relative amplitude of about 10^{-3} (Fig. 2 bottom).

Let us now discuss the influence of a nonlinearity, fixing for the moment the nonlinear parameter at $g=5$ (repulsive interaction) and $g=-5$ (attractive interaction). From Fig. 3 one can observe that the Bloch oscillations continue to exist, at least for the short times up to $t\approx 10T_B$ shown in the figure. In addition to the well known localization of $|\psi(x,t)|^2$ in the minima of the cosine potential, one observes a further filamentation which is particularly pronounced for an attractive interaction. As shown in Fig. 4, the amplitude of the oscillation decreases and the oscillation in the width strongly increases.

Also shown in Figs. 4 and 5 is the time dependence of the width Δx_t of the wave packet. In sharp contrast to the tiny oscillations of the width in the linear case (see Fig. 2) we find here very pronounced oscillations which are rapidly growing (as already described by Holthaus [16]). Such a phenomenon is known as *breathing* and is exhibited in the linear system by wave packets that are initially strongly localized

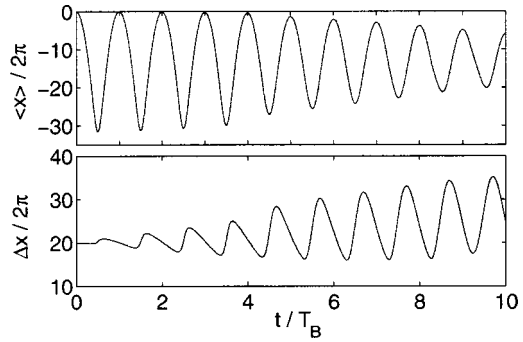

FIG. 5. Same as Fig. 4, but for an attractive nonlinearity $g=-5$.

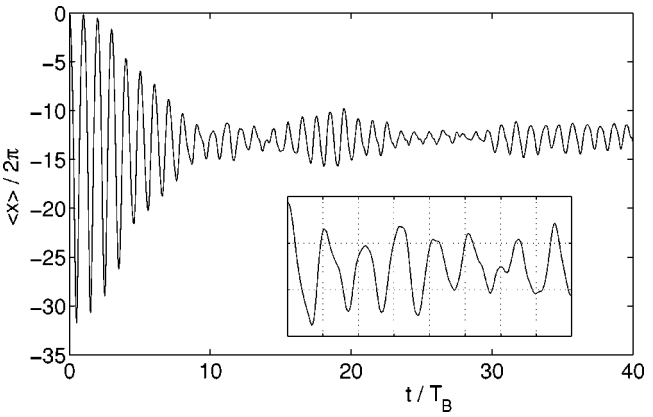

FIG. 6. Expectation value $\langle x\rangle_t$ of the position and width Δx_t for a repulsive nonlinearity $g=+10$. The inset shows a magnification of the time interval between $8T_B$ and $16T_B$.

in coordinate space [1,25]. Note that the oscillations of the width Δx_t for a repulsive and attractive nonlinearity are opposite to each other.

For a stronger nonlinearity $g=10$, as illustrated in Figs. 6 and 7, the Bloch oscillations are damped more strongly. However, the oscillation does not fade completely but shows a revival with a smaller amplitude after a shrinking to approximately two lattice periods. A corresponding behavior is observed for the width, where the breathing amplitude of the wave function first grows fast up to a time of about eight Bloch periods. After this time, the width remains limited and oscillates in the interval from 31 to 35 lattice periods.

Furthermore, the oscillation of $\langle x\rangle_t$ shows phase jumps that can be seen, e.g., in the inset of Fig. 6 at $t\approx 14T_B$. A similar behavior has also been described in [16]. This phase jump coincides with a minimum in the amplitude. These phenomena can be understood in terms of an expansion in Wannier-Stark basis functions as explained in the next section.

III. WANNIER-STARK BASIS SET EXPANSION

An alternative approach to a direct numerical integration of the GPE is an expansion in an adequate discrete basis such

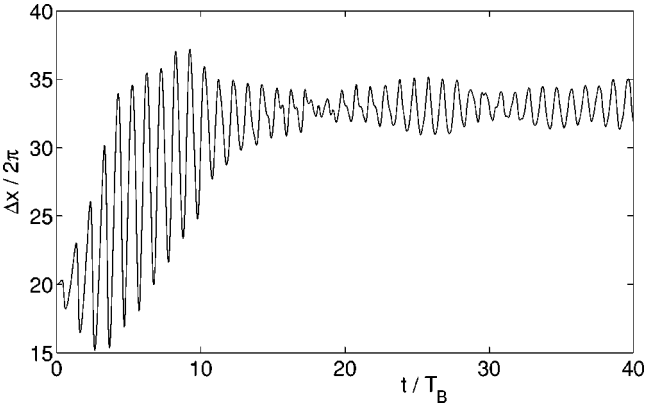

FIG. 7. Width Δx_t of the wave packet shown in Fig. 6 for a repulsive nonlinearity $g=+10$.

as for example the ground states of single potential wells [13,26]. In this work we adopt a different approach, following [14,18], and expand the wave function in the resonance eigenstates of the linear system, the so-called Wannier-Stark states $\Psi_{\alpha,n}(x)$ which are eigenstates of the linear Hamiltonian H_0:

$$H_0\Psi_{\alpha,n}(x) = \mathcal{E}_{\alpha,n}\Psi_{\alpha,n}(x), \tag{4}$$

where α is the ladder index and n is the site index. The energies form the Wannier-Stark ladder

$$\mathcal{E}_{\alpha,n} = \mathcal{E}_{\alpha,0} + 2\pi Fn. \tag{5}$$

The Wannier-Stark states extend over several periods of the potential (see remark [27] and review [5] for more information). This approach has proven to be extremely convenient to describe the dynamics in tilted optical lattices in the linear case, especially for higher field strengths [5,23].

Up to Sec. V, we will restrict the discussion to small field strengths F. Then one can neglect decay and Landau-Zener tunneling and use the lowest ladder $\alpha=0$ only; henceforth the index α is omitted. Also neglecting decay, the imaginary part of the energy $\mathcal{E}_n$ is set to zero. Plugging the expansion $\psi(x,t)=\Sigma_m c_m(t)\Psi_m(x)$ into the GPE (1) leads to a set of coupled ordinary differential equations:

$$i\hbar\sum_m \dot{c}_m\Psi_m = \sum_m (\mathcal{E}_0 + 2\pi Fm)c_m\Psi_m + g\sum_{klm} c_k^* c_l c_m \Psi_k^*\Psi_l\Psi_m. \tag{6}$$

The energy $\mathcal{E}_0$ only leads to a global phase factor and hence is omitted in the following. The Wannier-Stark states Ψ_n are orthogonal to their left eigenstates Ψ_m^L for $m\neq n$. Nevertheless, since we neglect the resonance properties of the system we can identify left and right eigenvectors, i.e., assume that H_0 is Hermitian. So multiplying Eq. (6) by Ψ_n^* and integrating yields

$$i\hbar\dot{c}_n = 2\pi Fnc_n + g\sum_{klm}\chi_{klm}^n c_k^* c_l c_m, \tag{7}$$

with the coupling tensor

$$\chi_{klm}^n = \int \Psi_n^*(x)\Psi_k^*(x)\Psi_l(x)\Psi_m(x)dx, \tag{8}$$

which is symmetric under the exchange of its first and last two indices. Due to the discrete translational invariance of the Wannier-Stark states $\Psi_n(x)=\Psi_0(x-2\pi n)$ one finds

$$i\hbar\dot{c}_n = 2\pi Fnc_n + g\sum_{klm}\chi_{klm} c_{k+n}^* c_{l+n} c_{m+n}, \tag{9}$$

defining $\chi_{klm}\equiv\chi_{klm}^0$.

Though not suited for direct numerical calculations because of the triple infinite sum, Eq. (9) provides a basis for further approximations. In the following we will reduce it to a simple integrable model, which nevertheless captures important features of the dynamics. To this end we decompose the coefficients c_n into phase and amplitude

$$c_n = \sqrt{\rho_n}e^{i\varphi_n}. \tag{10}$$

The imaginary parts of the coupling tensor χ_{klm} are negligible and so one arrives at the coupled equations

$$\hbar\dot{\varphi}_n = -2\pi Fn - g\rho_n\sum_{klm}\chi_{klm}\left(\frac{\rho_{k+n}\rho_{l+n}\rho_{m+n}}{\rho_n^3}\right)^{1/2} \times\cos(\varphi_{l+n}+\varphi_{m+n}-\varphi_{k+n}-\varphi_n), \tag{11}$$

$$\hbar\dot{\rho}_n = 2g\rho_n^2\sum_{klm}\chi_{klm}\left(\frac{\rho_{k+n}\rho_{l+n}\rho_{m+n}}{\rho_n^3}\right)^{1/2} \times\sin(\varphi_{l+n}+\varphi_{m+n}-\varphi_{k+n}-\varphi_n). \tag{12}$$

If the initial state is broad, populating about 20 wells, the amplitudes $\rho_n(t=0)$ are small. Because of $\dot{\rho}_n\sim\rho_n^2$, this implies that the amplitudes ρ_n change only slowly in time compared to the phases φ_n and can be assumed to be constant.

Furthermore we reduce the expression for $\dot{\varphi}_n$ to the most important contributions. Numerically examining the χ_{klm} shows that the dominating terms are χ_{000}, $\chi_{kk0}=\chi_{k0k}$, and χ_{0kk}, which is not unexpected considering Eq. (8). It can also be argued (and verified numerically) that the terms in Eq. (11) that have a nonzero argument of the cosine have little importance, as their contributions average out. This leaves the terms including χ_{000} and $\chi_{kk0}=\chi_{k0k}$ and finally leads to

$$\hbar\dot{\varphi}_n = -2\pi Fn - g\gamma_n\rho_n \tag{13}$$

with

$$\gamma_n = \chi_{000} + 2\sum_{k\neq 0}\chi_{k0k}\frac{\rho_{n+k}}{\rho_n}. \tag{14}$$

Equations (13) are integrated to

$$\rho_n(t) = \rho_n(0), \quad \varphi_n(t) = \omega_n t, \tag{15}$$

with

$$\hbar\omega_n = -2\pi Fn - g\gamma_n\rho_n. \tag{16}$$

Note that this solution is exact for $g=0$. Numerical calculations show that one can safely neglect the dependence of γ_n on the index n and set $\gamma_n\approx\gamma$. For the given parameters Eq. (14) yields $\gamma_n\geqslant\gamma_0=0.278$. However, the best fit with the results from a wave packet propagation are obtained for $\gamma=0.15$.

This admittedly quite crude approximation shows very good agreement with an exact numerical solution. In Figs. 8 and 9 the approximation (15) is compared with the results obtained by a wave packet propagation using the split-operator method [24]. A normalized Gaussian initial distribution with coefficients

$$c_n \sim e^{-n^2/4\sigma^2}, \quad \sigma = \tilde{\sigma}/2\pi = 20, \tag{17}$$

is used which closely resembles a Gaussian wave packet projected onto the lowest Bloch band in configuration space. The dynamics for a moderate nonlinearity $g=1$ is well described by Eq. (15), only the growth of the width is somewhat underestimated. For $g=10$ the approximation (15) becomes less accurate. In particular it overestimates the revival

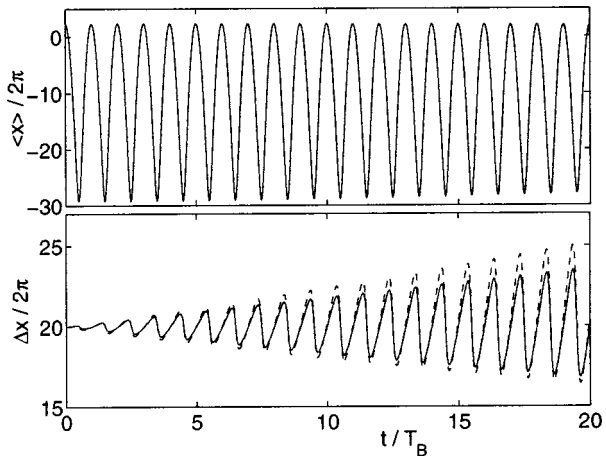

FIG. 8. Bloch oscillations: Expectation value of position $\langle x\rangle_t$ of the wave packet for a moderate nonlinearity $g=1$. The propagation was done with the split-operator method (dashed line) respectively with approximation (15) (solid line).

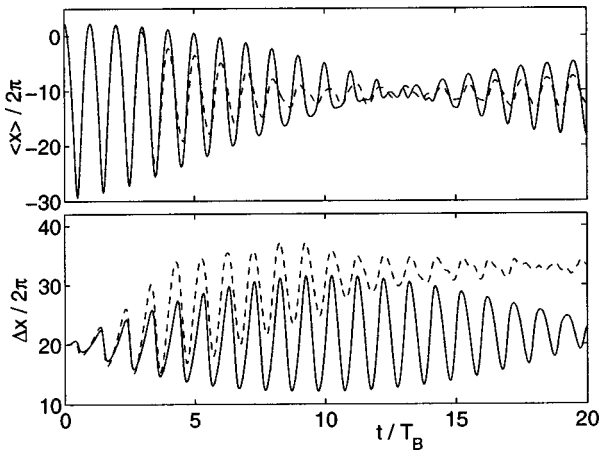

FIG. 9. As Fig. 8, but for a strong nonlinearity $g=10$.

of the Bloch oscillation and underestimates the growth of the width of the wave packet. However, it still captures the important features at least qualitatively: the decay and revival of the oscillations, the phase jump around $t=14T_B$ and the breathing of the wave function.

The systematic growth of the width of the wave packet is mainly due to a broadening of the amplitude distribution ρ_n and therefore clearly not included in approximation (15). Similarly, the filamentation of the wave packet (cf. Fig. 3) is also due to the dynamics of the amplitude distribution ρ_n and hence not included in our simple model.

To discuss the broadening of the wave function we briefly reintroduce the time dependence of the ρ_n. Again we reduce the triple sum to keep the calculations feasible. Note that the terms are oscillating due to the sine. Using approximation (15) we see that for $k=l+m$ the terms proportional to F in the argument of the sine cancel and hence the sine oscillates most slowly. Thus we approximate the dynamics of the amplitudes ρ_n by

$$\hbar\dot{\rho}_n \approx 2g\rho_n^2 \sum_{l,m} \chi_{l+m,l,m} \left(\frac{\rho_{l+m+n}\rho_{l+n}\rho_{m+n}}{\rho_n^3} \right)^{1/2} \times \sin(\varphi_{l+n} + \varphi_{m+n} - \varphi_{l+m+n} - \varphi_n), \tag{18}$$

where the sum can be truncated at $|l|,|m|=30$. Equation (18) for ρ and Eq. (13) for φ are now solved numerically with $\gamma=0.15$ and the initial condition (17). The results displayed in Fig. 10 show that this model captures the growth of the width of the wave packet. We will, however, not go into details here and return to the approximation (15) to discuss the dynamics of Bloch oscillations.

IV. ANALYSIS OF THE DYNAMICAL BEHAVIOR

Further insight can be provided by a closer look at the dynamics of the wave function in momentum space. This can be achieved with the approximate time evolution of the expansion coefficients c_n derived in the previous section.

First we briefly reconsider the linear case. For $g=0$ Eqs. (15) reduce to

$$\rho_n(t) = \rho_n(t=0) \quad \text{and} \quad \varphi_n(t) = -2\pi Fnt/\hbar. \tag{19}$$

The Wannier-Stark functions [27] Ψ_n are related by a spatial translation $\Psi_n(x)=\Psi_0(x-2\pi n)$. In momentum space this reads

$$\Psi_n(k) = e^{-i2\pi nk}\Psi_0(k) \tag{20}$$

and the time evolution of the wave function in momentum space is

$$\psi(k,t) = \Psi_0(k)\sum_n \sqrt{\rho_n}\exp[-i2\pi n(k+Ft/\hbar)] \sim \Psi_0(k)\widetilde{C}(k+Ft/\hbar), \tag{21}$$

neglecting a global phase. Thus the wave function is the product of a time-independent function $\Psi_0(k)$ and the discrete Fourier transformation $\widetilde{C}(k)$ of the amplitudes $\sqrt{\rho_n}$, evaluated at the point $k+Ft/\hbar$.

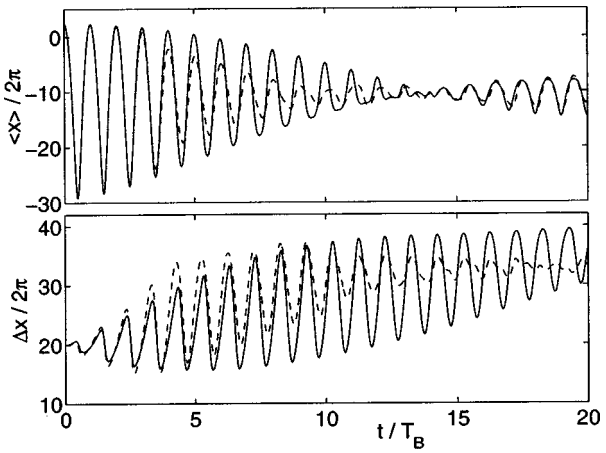

FIG. 10. Bloch oscillations for a strong nonlinearity $g=10$. The propagation was done with the split-operator method (dashed line) and with approximation (18) (solid line).

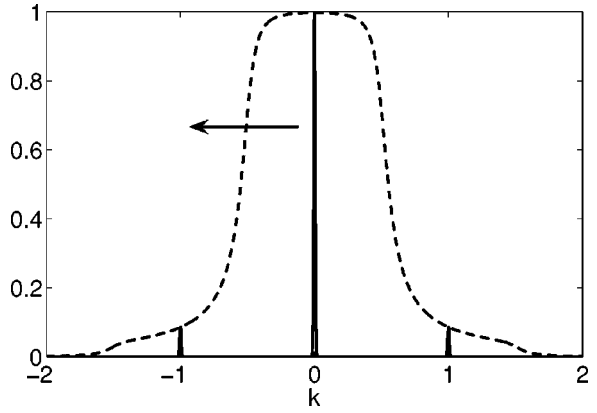

FIG. 11. Bloch oscillations in momentum space. The wave function $|\psi(k,t)|$ shown for $t=0$ (solid line) moves uniformly under the envelope of the Wannier-Stark function $|\Psi_0(k)|$ (dashed line).

The function $\tilde{C}(k)$ is periodic in momentum space: $\tilde{C}(k+n)=\tilde{C}(k)$ for $n\in\mathbb{Z}$. Thus the function $\tilde{C}(k+Ft/\hbar)$ is periodic in time with the Bloch period $T_B=\hbar/F$. For a broad Gaussian distribution of the amplitudes ρ_n the discrete Fourier transform $\tilde{C}(k)$ is a comb function with narrow peaks at $k=n$.

So one arrives at a simple view of the dynamics in momentum space: The comb function $\tilde{C}(k)$ moves uniformly under the envelope $\Psi_0(k)$, as illustrated in Fig. 11. In coordinate space this periodic motion appears as a Bloch oscillation [1].

In the nonlinear case one has to evaluate

$$\psi(k,t)=\Psi_0(k)\sum_n \sqrt{\rho_n}\exp\{-i[2\pi nk-\varphi_n(t)]\}=\Psi_0(k)\tilde{C}(k,t) \tag{22}$$

instead of Eq. (21). The time evolution of the phases is approximated according to Eq. (15):

$$\varphi_n(t)=\omega_n t \quad \text{with } \hbar\omega_n=-2\pi Fn-g\gamma\rho_n, \tag{23}$$

and the amplitudes are assumed to be Gaussian

$$\rho_n(t)=\rho_n\sim e^{-n^2/2\sigma^2}. \tag{24}$$

As in the linear case, the static field term $-2\pi Fn$ in Eq. (23) for the frequency leads to a uniform motion of the function $\tilde{C}(k,t)$ in momentum space. The nonlinear term $-g\gamma\rho_n$ leads to a dephasing of the coefficients c_n and broadens the Fourier transform $\tilde{C}(k,t)$. This dephasing causes a damping of the Bloch oscillations in coordinate space.

The oscillations of the width Δx_t, the breathing, can also be understood with this approach. In the linear case such breathing occurs for wave functions that are initially strongly localized in coordinate space and thus have a broad momentum distribution. As explained, the nonlinear term leads to a broadening of the function $\tilde{C}(k,t)$ and hence to a broadening of the wave function in momentum space and breathing in coordinate space. For even longer times the coefficients dephase completely and the oscillations in both the position and the width are damped.

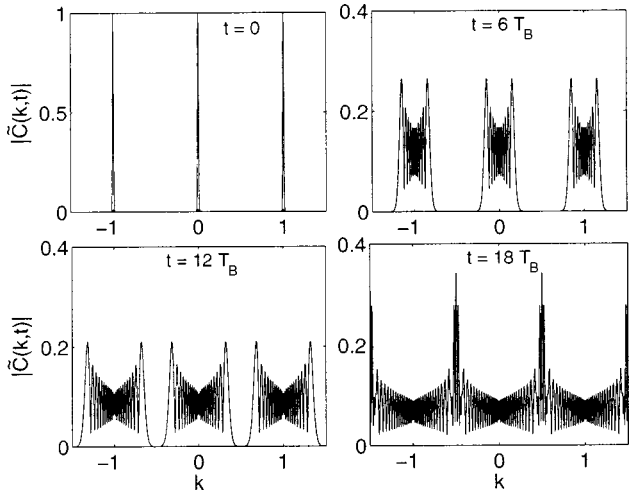

FIG. 12. Time evolution of the function $\tilde{C}(k,t)$ in Eq. (22) for $g=10$. The function $\tilde{C}$ is scaled as $\tilde{C}(0,0)=1$.

In order to understand the revivals and the phase jumps in the oscillations of $\langle x\rangle_t$, we need to look at the time evolution of the function $\tilde{C}(k,t)$. In Fig. 12 the function $|\tilde{C}(k,t)|$ for $g=10$ is plotted at times $t=0$, $t=6T_B$, $t=12T_B$, and $t=18T_B$. The dynamics of the expansion coefficients was calculated with Eq. (15) [Eq. (23)]. One observes that the initially narrow peaks are broadened and an oscillatory structure develops with two maxima at the edges of the band populated by $|\tilde{C}(k,t)|$. These maxima eventually merge, leading to a revival of the Bloch oscillations. The new maximum after the merger is displaced by $\Delta k=0.5$ in comparison to the linear case and hence the phase of the Bloch oscillations is reversed. This maximum broadens again, leading to a periodic breakdown and revival. The phase of the Bloch oscillations is reversed after each breakdown and the amplitudes of the revivals decrease. However, these further revivals are observed only within the approximation (15) and *not* in a wave packet propagation.

Now we consider the time dependence of the expectation values of position and width. These quantities can be evaluated analytically in the linear case $g=0$ using a tight-binding approximation [1,25]. In this approximation the expectation value of the position oscillates harmonically with the Bloch frequency ω_B,

$$\langle x\rangle_t=\overline{x}+A\cos(\omega_B t) \tag{25}$$

and amplitude

$$A=\frac{\Delta}{2F}e^{-2\pi^2\Delta p^2/\hbar^2}, \tag{26}$$

where Δp is the width in momentum space and Δ is the bandwidth of the dispersion relation $E(\kappa)$ in the field-free case. For a small nonlinearity the broadening of the wave function in momentum space due to the nonlinearity happens

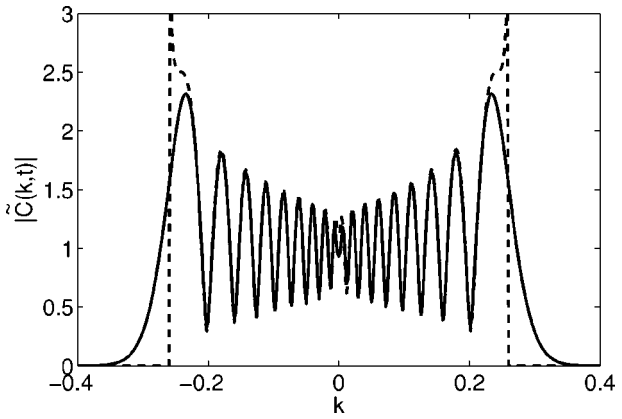

FIG. 13. Function $|\tilde{C}(k,t)|$ [Eq. (27)] for $gt=90T_B$ and $\gamma=0.15$. The integral was evaluated numerically (solid line) and using the stationary phase method (dashed line).

slowly compared to the Bloch oscillations. Thus we can assume that $\langle x\rangle_t$ still executes damped harmonic oscillations with the amplitude (26), where the damping is determined by the slowly increasing momentum width Δp_t.

According to Eq. (22) we can estimate the momentum width Δp_t by the width of the peaks of the function $\tilde{C}(k,t)$. For a broad distribution of the coefficients c_n, as assumed throughout this paper, the sum in Eq. (22) can be replaced by an integral:

$$\tilde{C}(k,t) = \int_{-\infty}^{+\infty} \sqrt{\rho_n}\exp\{-i[2\pi nk - \varphi_n(t)]\}dn. \tag{27}$$

This expression is valid for $|k|<0.5$, otherwise $\tilde{C}(k,t)$ is determined by its periodicity. The amplitudes ρ_n and phases $\varphi_n(t)$ are approximated by Eq. (15), where the amplitudes ρ_n are normalized as

$$\rho_n = \frac{1}{\sqrt{2\pi\sigma^2}} e^{-n^2/2\sigma^2}. \tag{28}$$

We note that $\tilde{C}(k,t)$ depends on the momentum k only through the expression $\tilde{k}=k+Ft/\hbar$, reflecting the uniform motion in momentum space due to the static field:

$$\tilde{C}(\tilde{k}) = \frac{1}{\sqrt[4]{2\pi\sigma^2}} \int_{-\infty}^{+\infty} e^{-n^2/4\sigma^2} e^{-i(2\pi\tilde{k}n+\beta e^{-n^2/2\sigma^2})} dn \tag{29}$$

with $\beta=\gamma gt/(\sqrt{2\pi}\sigma\hbar)$.

The integral (27) can be evaluated using the stationary phase approximation. However, there exists only a finite $\tilde{k}$ interval for which stationary points exist. For $|\tilde{k}|>|k_c|$ with

$$k_c = \frac{\beta}{2\pi\sigma e^{1/2}} \tag{30}$$

the integral vanishes in the simple stationary phase approximation [30]. For $|\tilde{k}|<|k_c|$ one obtains

$$\tilde{C}(k,t) \approx \left(\frac{2\pi\sigma^2}{\beta^2}\right)^{1/4} \left(\frac{e^{i\zeta_+}}{\sqrt{1-z_+}} + \frac{e^{i\zeta_-}}{\sqrt{1-z_-}}\right), \tag{31}$$

where $z_\pm$ are the two solutions of the equation

$$ze^{-z} = (2\pi\sigma\tilde{k}/\beta)^2 \tag{32}$$

and the abbreviations $\zeta_\pm = -2\pi\sigma\tilde{k}(z_\pm^{+1/2} + z_\pm^{-1/2})$ were used. As an example the function $|\tilde{C}(k,t)|$ is plotted in Fig. 13 for $gt=90T_B$ and $\gamma=0.15$.

Estimating the momentum width as $\Delta p \approx \hbar|k_c|$ one arrives at

$$\Delta p_t \approx \frac{|\gamma g|}{(2\pi)^{3/2}\sigma^2 e^{1/2}} t. \tag{33}$$

Thus the damped Bloch oscillations in coordinate space are described by

$$\langle x\rangle_t \approx \overline{x} + \frac{\Delta}{2F}\exp\left(-\frac{\gamma^2 g^2 t^2}{4\pi e\hbar^2\sigma^4}\right)\cos(\omega_B t) \tag{34}$$

according to Eq. (25). The amplitude decreases exponentially with $-g^2t^2$ in agreement with the estimate given in [13].

Furthermore we can calculate approximately the time up to the first rephasing of the coefficients and thus the first revival of the Bloch oscillations. This revival occurs if the outer peaks of $\tilde{C}(k,t)$ meet at $k=n+1/2$, $n\in\mathbb{Z}$, as illustrated in Fig. 12. Therefore the first rephasing and revival occurs for $k_c=0.5$ which yields a revival time

$$t_{\text{rev}} \approx \frac{(2\pi)^{3/2} e^{1/2}\hbar\sigma^2}{2|\gamma g|}. \tag{35}$$

For $g=10$ and $\gamma=0.15$ one obtains

$$t_{\text{rev}} \approx 17T_B, \tag{36}$$

in reasonable agreement with the revival of Bloch oscillations observed numerically for the wave packet propagation shown in Fig. 6.

For very long times the coefficients c_n dephase completely. We can therefore estimate the position expectation value by approximating the wave function as an incoherent sum of the basis states. Assuming that the amplitudes ρ_n are constant in time according to Eq. (13) one has

$$\langle x\rangle = \sum_n \rho_n \langle\Psi_n|x|\Psi_n\rangle. \tag{37}$$

Using the translational properties of the Wannier-Stark states (cf. [5]) one arrives at

$$\langle x\rangle_\infty \approx \langle\Psi_0|x|\Psi_0\rangle + 2\pi\sum_n n\rho_n. \tag{38}$$

The amplitudes of the initial state (17) are symmetric around $n=0$ and hence this approximation yields $\langle x\rangle_\infty \approx \langle\Psi_0|x|\Psi_0\rangle = -10.5\times 2\pi$. This estimation fairly agrees with the numerical results displayed in Fig. 6. As argued above, the systematic growth of the width of the wave packet is mainly due to a broadening of the amplitude distribution ρ_n and hence cannot be explained using the simple model discussed here.

V. STRONG STATIC FIELD AND DECAY

An expansion into Wannier-Stark resonances is also very helpful in order to understand the dynamics and decay in strong static fields. In the following we will discuss the dynamics for the parameters $\hbar = 3.3806$ and $F = 0.0661$, corresponding to the experiment of Anderson and Kasevich [7]. A detailed discussion of this experiment in terms of Wannier-Stark resonances, but neglecting the nonlinearity, can be found in [23]. Thus we will only briefly discuss the influence of the nonlinearity on the pulse shape.

For a field strength of $F = 0.0661$ decay cannot be neglected any longer. One has to take into account that the resonance states eventually diverge exponentially for x or $k \to -\infty$. Hence, a wave function of the form (22) is not normalizable. Nevertheless, the restriction to the ground Wannier-Stark ladder is still sufficient.

As described in [23] (see also remark [27]) one can solve the problem of normalization by introducing truncated resonance states defined by

$$\Psi_n^K(k) = \Theta(k + K)\Psi_n(k). \tag{39}$$

The Heaviside function $\Theta(k+K)$ truncates the resonances at $-K$. Provided that $|K|$ is large enough, the time evolution of these states is given by

$$\Psi_n^K(k,t) = \Theta(k + K + Ft/\hbar)\Psi_n(k,t). \tag{40}$$

If the support of the initial wave function is bounded in momentum space by $|k| < |K|$, we can expand it into a basis of truncated resonances. The dynamics of this state is then given by

$$\psi(k,t) = \Theta(k + K + Ft/\hbar)\Psi_0(k,t)\widetilde{C}(k,t), \tag{41}$$

with $\Psi_0(k,t) = \exp(-i\mathcal{E}_0 t/\hbar)\Psi_0(k)$ instead of Eq. (22).

For a coherent initial distribution of a sufficient width $c_n \sim \exp[-n^2/(2\sigma)^2]$ with $\sigma \gg 1$, the function $\widetilde{C}(k,t)$ is a comb function in the linear case, leading to a pulsed output. The pulse shape given by the function $\widetilde{C}$ broadens and deforms under the influence of the nonlinearity as described in the previous section (cf. Fig. 12). This deformation is directly observable in the pulsed output.

This is demonstrated in Fig. 14 for a coherent initial distribution $c_n \sim \exp(-n^2/4\sigma^2)$ with a width of $\sigma = 15/2$. The time evolution was again calculated using a split-operator method. The wave function $|\psi(k,t)|^2$ is plotted at a time $t = 9.1T_B$ for four different values of the nonlinearity $g = 0$, -5, 5, and 10. The broadening of the peaks with increasing $|g|$ and the characteristic double-peak structure can clearly be seen.

The resulting wave function in coordinate space is a sequence of pulses at the points

$$x = x_0 - \frac{F}{2}(t + jT_B)^2, \tag{42}$$

with $x_0 = E_0/F$ and $j \in \mathbb{Z}$. These pulses are accelerated just like classical particles in a static field, as observed in the experiment [7]. The pulse shape is approximately described by the discrete Fourier transform of $\widetilde{C}$ [23]. Thus one also finds a characteristic deformation of the pulses in coordinate space.

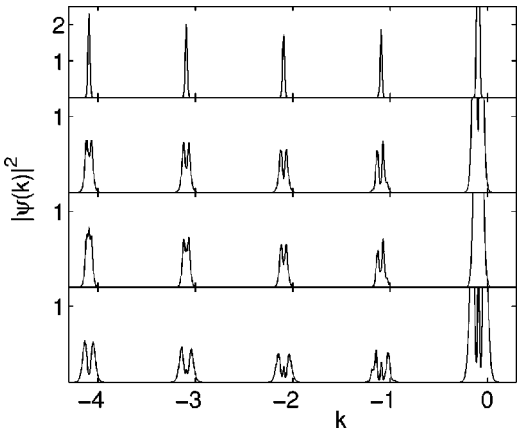

FIG. 14. Pulsed output for different nonlinearities $g = 0$, -5, 5, and 10 (from top to bottom). The wave function $|\psi(k,t)|^2$ is displayed for $t = 9.1T_B$.

VI. CONCLUSIONS

In this article we first investigated Bloch oscillations of BECs by numerical solutions of the Gross-Pitaevskii equation and demonstrated a revival of Bloch oscillations after an initial breakdown. These findings have been further analyzed via discretizing the GPE in a Wannier-Stark basis set expansion. Using these resonance states one can easily compare the linear and nonlinear cases. This comparison leads to a better understanding of the nonlinear features of BECs in optical lattices. It allows us to derive a simple integrable model (15) which can explain the nonlinear phenomena of breakdown and revival of the Bloch oscillations. This approach, unlike the tight-binding approximation, works as well for strong Stark fields.

Many interesting questions are left open and deserve future studies, as for example the following. (a) The effects induced by the nonlinearity for Bloch oscillations in two-dimensional lattices, where recently novel effects concerning the extreme sensitivity on the field direction with respect to the lattice have been found [3,28]. (b) For BECs in tilted optical lattices a classically chaotic behavior has been reported [14]. These interesting findings deserve further studies, for example the correspondence of the emergence of chaos with the loss of stability of the GPE solutions. (c) It is an entirely open question how the nonlinearity influences the behavior of a driven Wannier-Stark system, e.g., the stabilizing phenomena found for an additional harmonic driving [5,29].

ACKNOWLEDGMENTS

Support from the Deutsche Forschungsgemeinschaft as well as from the Volkswagen Foundation is gratefully acknowledged. We thank Jean-Claude Garreau, Andrey Kolovsky, and Andreas Buchleitner for providing results prior to publication.

[1] T. Hartmann, F. Keck, H. J. Korsch, and S. Mossmann, New J. Phys. **6**, 2 (2004).
[2] A. R. Kolovsky and H. J. Korsch, Phys. Rev. A **67**, 063601 (2003).
[3] D. Witthaut, F. Keck, H. J. Korsch, and S. Mossmann, New J. Phys. **6**, 41 (2004).
[4] A. R. Kolovsky and H. J. Korsch, J. Mod. Phys. **18**, 1235 (2004).
[5] M. Glück, A. R. Kolovsky, and H. J. Korsch, Phys. Rep. **366**, 103 (2002).
[6] J. Feldmann, K. Leo, J. Shah, D. A. B. Miller, J. E. Cunningham, T. Meier, G. von Plessen, A. Schulze, P. Thomas, and S. Schmitt-Rink, Phys. Rev. B **46**, R7252 (1992).
[7] B. P. Anderson and M. A. Kasevich, Science **282**, 1686 (1998).
[8] M. L. Chiofalo and M. P. Tosi, Phys. Lett. A **268**, 406 (2000).
[9] K. Berg-Sørensen and K. Mølmer, Phys. Rev. A **58**, 1480 (1998).
[10] Dae-Il Choi and Qian Niu, Phys. Rev. Lett. **82**, 2002 (1999).
[11] Biao Wu and Qian Niu Phys. Rev. A **61**, 023402 (2000).
[12] Biao Wu and Qian Niu, New J. Phys. **5**, 104 (2003).
[13] A. Trombettoni and A. Smerzi, Phys. Rev. Lett. **86**, 2353 (2001).
[14] Q. Thommen, J. C. Garreau, and V. Zehnlé, Phys. Rev. Lett. **91**, 210405 (2003).
[15] A. R. Kolovsky and A. Buchleitner (unpublished).
[16] M. Holthaus, J. Opt. B: Quantum Semiclassical Opt. **2**, 589 (2000).
[17] J. Javanainen, Phys. Rev. A **60**, 4902 (1999).
[18] Q. Thommen, J. C. Garreau, and V. Zehnlé, J. Opt. B: Quantum Semiclassical Opt. **6**, 301 (2004).
[19] L. Fallani, L. De Sarlo, J. E. Lye, M. Modugno, R. Saers, C. Fort, and M. Inguscio, Phys. Rev. Lett. **93**, 140406 (2004).
[20] Biao Wu and Qian Niu, Phys. Rev. A **64**, 061603(R) (2001).
[21] J. Liu, B. Wu, and Q. Niu, Phys. Rev. Lett. **90**, 170404 (2003).
[22] C. Menotti, A. Smerzi, and A. Trombettoni, New J. Phys. **5**, 112 (2003).
[23] M. Glück, F. Keck, and H. J. Korsch, Phys. Rev. A **66**, 043418 (2002).
[24] M. D. Feit, J. A. Fleck, Jr., and A. Steiger, J. Comput. Phys. **47**, 412 (1982).
[25] H. J. Korsch and S. Mossmann, Phys. Lett. A **317**, 54 (2003).
[26] F. Kh. Abdullaev, B. B. Baizakov, S. A. Darmanyan, V. V. Konotop, and M. Salerno, Phys. Rev. A **64**, 043606 (2001).
[27] Though not important for weak fields, it should be noted that the Wannier-Stark states are not normalizable because of their exponentially increasing tail at $x \to -\infty$. In practice, this can be circumvented by a cutoff in coordinate space or momentum space. For the stronger fields considered in Sec. V this truncation must be explicitly taken into account.
[28] S. Mossmann, A. Schulze, D. Witthaut, and H. J. Korsch, e-print quant-ph/0409114, J. Phys. A (to be published).
[29] M. Glück, A. R. Kolovsky, and H. J. Korsch, Europhys. Lett. **51**, 255 (2000).
[30] If desired, the stationary phase points can be continued into the complex plane leading to an exponential decay.